Letter

Nonlinear Fourier transform for analysis of optical spectral combs

S. K. Turitsyn,[1,2] I. S. Chekhovskoy,[1] and M. P. Fedoruk[1]

[1]*Novosibirsk State University, Novosibirsk 630090, Russia*

[2]*Aston Institute of Photonic Technologies, Aston University, Birmingham B4 7ET, United Kingdom*

(Received 9 August 2020; accepted 20 January 2021; published 18 February 2021)

The nonlinear Fourier transform (NFT) is used to characterize the optical combs in the Lugiato-Lefever equation with both anomalous and normal dispersion. We demonstrate that the NFT signal processing technique can simplify analysis of the formation of dissipative dark solitons and regimes exploiting modulation instability for a generation of coherent structures, by approximating the comb with several discrete eigenvalues, providing a platform for the analytical description of dissipative coherent structures.

DOI: 10.1103/PhysRevE.103.L020202

Optical spectral comb technology enables a range of existing and emerging applications (see [1–7] and references therein). Due to their chip-scale size and potential for integration, microresonator frequency combs are attractive for the generation of equally spaced, coherent (phase-locked) spectral lines, which is of particular interest for superchannel based optical communications. Multiterabit per second coherent transmission has recently been demonstrated using both dissipative solitons and dark pulses in microresonators [8,9]. The optical comb technology is based on the nonlinear science underlying the building of coherent optical structures that ensure phase locking of spectral modes in the resonator.

Localized coherent structures and patterns formed from noise or unstable homogeneous states occur in a wide range of applications in physics and biology. Despite a great variety of these applications, they often have similar underlying mathematical models that offer a generic platform for new methods of analysis of localized temporal or spatial nonlinear waves. In this Letter, we demonstrate applications of the nonlinear science method, i.e., inverse scattering transform (IST), also known as the nonlinear Fourier transform (NFT), to the characterization of optical combs in several practically important configurations.

The master model governing the average evolution of the envelope of the optical field in a nonlinear fiber resonator or microresonator (see, for more details, [1–7,10,11] and references therein) reads

$$i\frac{\partial \Psi}{\partial T} - \frac{\beta}{2}\frac{\partial^2 \Psi}{\partial \tau^2} + |\Psi|^2\Psi = (-i + \zeta_0)\Psi + if. \qquad (1)$$

Here, $\Psi(T, \tau)$ is a slowly varying field amplitude, T is a normalized time corresponding to the cavity round trips, τ is a dimensionless longitudinal coordinate related to the angular characteristic inside the microresonator (or the local time characteristic in the case of a fiber resonator), ζ_0 is the normalized laser detuning between the pump laser frequency and the cold-cavity resonance frequency, and f is the normalized pump field amplitude; $\beta = \mp 1$ corresponds to, respectively, focusing or defocusing cases (anomalous or normal dispersion in the context of fiber-optic applications). Equation (1) is a mean-field model, widely known as the Lugiato-Lefever equation (LLE) [12], and was originally introduced in the context of plasma physics in [13] and first derived in the temporal domain in [14]. The left-hand side of Eq. (1) (assuming that the right-hand side is zero) presents the nonlinear Schrödinger equation (NLSE) that is integrable by IST [15,16].

The IST (NFT) method in application to NLSE is well documented and details can be found, for instance, in [15–18]; therefore, here we only briefly remind the reader of the key facts that will be used below. We limit IST (NFT) consideration by fields $\Psi(T, \tau)$ decaying at $\tau \to \pm\infty$ for all T. The NLSE solutions $\Psi(T, \tau)$ are linked to the spectrum of a linear operator—the Zakharov-Shabat spectral problem (ZSSP) for potential $\Psi(T, \tau)$ and a spectral parameter $\lambda = \xi + i\eta$, as follows:

$$\frac{\partial u}{\partial \tau} = -i\lambda u + \Psi(T, \tau)v, \qquad \frac{\partial v}{\partial \tau} = \beta\Psi^*(T, \tau)u + i\lambda v. \qquad (2)$$

For $\beta = -1$, the eigenvalue problem is non-Hermitian (ZSSP1), and for $\beta = 1$, the operator is Hermitian (ZSSP2). Any solution of the NLSE $\Psi(T, \tau)$ with $\beta = -1$ can be presented through the corresponding nonlinear spectrum of the ZSSP1 that, in general, includes (i) a continuous spectrum that is defined on the real axis of the complex plane $\lambda = \xi$ by the complex function $r(\xi)$, and (ii) a discrete spectrum that is described by $4 \times N$ real parameters (the set of complex-valued eigenvalues $\{\lambda_n\}$ having a positive imaginary part together with the complex-valued norming constants $\{r_n\}$). The discrete eigenvalues correspond to a soliton component of the field $\Psi(T, \tau)$, with N being the total number of solitons. For the field $\Psi(T, \tau)$ that consists of a set of well-separated solitons, each eigenvalue λ_n specifies the soliton parameters: amplitude $2\mathrm{Im}(\lambda_n)$, frequency $-2\mathrm{Re}(\lambda_n)$, position $T_n = \ln[|r_n|/(2\mathrm{Im}\lambda_n)]/(2\mathrm{Im}\lambda_n)$, and phase $\varphi_n = -\arg(ir_n)$.

For the case $\beta = -1$, the field energy can be presented as a sum of continuous (dispersive waves) and discrete (solitons) spectra of ZSSP1,

$$\int_{-\infty}^{\infty} |\Psi(T,\tau)|^2 d\tau = \sum_{n=1}^{N} 4\eta_n + \frac{1}{\pi}\int_{-\infty}^{\infty} \ln[1+|r(\xi)|^2] d\xi, \tag{3}$$

where the left side of the equality corresponds to the energy calculated in the temporal domain $E_t(T)$, while the right side includes a contribution of the discrete spectrum energy $E_d(T)$ and the continuous spectrum $E_c(T)$.

The initial idea (e.g., presented in [19–22]) behind using IST (NFT) beyond the traditional integrable systems was to exploit the fact that for some nonintegrable (e.g., dissipative) models, the Hamiltonian part of these equations is NLSE, and, thus, one can expect that the IST (NFT) might still be a useful tool for analysis of the whole (non-Hamiltonian) systems. The term NFT stresses the analogy with the traditional Fourier transform that is ubiquitous in science and engineering. Fourier transform might be useful in simplifying the description of complex objects by presenting them via spectral harmonics. It was shown in [19,21,22] that in a similar manner, IST (NFT) can be employed not only for solving integrable equations, but also for the characterization of localized coherent structures in dissipative systems in the anomalous dispersion regime. Note that in [23], NFT with periodic boundary conditions was applied for analysis of static (output) optical comb profiles in the LLE model. However, in the case of periodic NFT, localized structures have been presented by a large number of discrete eigenvalues, which does not allow one to reduce the number of the effective degrees of freedom compared to conventional Fourier transform.

In this Letter, we demonstrate additional features and different applications of NFT compared to the initial idea [19–21]. We advance this emerging signal processing technique by introducing the following applications of NFT to the characterization of the dynamics of coherent structures during the generation of optical combs: (i) We apply NFT based on the Zakharov-Shabat spectral problem with $\beta = -1$ to the nonlinear system with $\beta = 1$, to stress that we do not use the spectral problem for solving the equation, but for processing of the signal. This is, evidently, a dramatic departure from the traditional IST, where the sign of β must be the same for the NLSE and ZSSP used for its integration. (ii) We demonstrate how NFT can be used in the case of pulsed pumping waves. (iii) We characterize, in terms of the NFT spectrum, the generation of an optical comb through modulation instability-induced oscillations when detuning is switched to ensure a shift from an unstable cw background to stable one. (iv) We demonstrate that a steady-state dissipative dark soliton can be well approximated analytically by the expression for N-soliton solutions of NLSE with a small number of parameters.

A typical solution of Eq. (1) includes a cw background $\Psi_0(T)$ and a solitonic part $\Psi_1(T,\tau)$. Evolution of the cw background $\Psi_0(T)$ is given by

$$i\frac{\partial \Psi_0}{\partial T} + |\Psi_0|^2\Psi_0 = (-i+\zeta_0)\Psi_0 + if. \tag{4}$$

There are well-known solutions of (4) in the form of a constant cw background that can be found by solving Eq. (4) with $\frac{\partial \Psi_0}{\partial T} = 0$, yielding an algebraic equation on the stationary background $I_0 = |\Psi_0|^2$: $I_0^3 - 2\zeta_0 I_0^2 + (1+\zeta_0^2)I_0 - f^2 = 0$. There are three real roots, when the condition $f_-^2 \leqslant f^2 \leqslant f_+^2$ is satisfied, where

$$f_\pm^2 = \frac{2}{27}\left[\zeta_0(\zeta_0^2+9) \pm \sqrt{(\zeta_0^2-3)^3}\right],$$

and one real root otherwise. When $\zeta_0 < \sqrt{3}$, only one real root exists [11].

When localized structures that define the comb have a timescale much less than the round trip, it is possible to separate the dynamics of the stable background field with nonzero boundary conditions (in τ) from the evolution of the localized in time (vanishing boundary conditions) soliton content. This is possible when, at large $|\tau|$, localized structures do not affect the cw background. Considering the solution of the master model (1) as a sum of the uniform (in τ) background Ψ_0 that depends only on T and the soliton (localized in τ) component Ψ_1, we can separate the evolution in T of Ψ_0 governed by Eq. (4), and the dynamics of the field Ψ_1:

$$i\frac{\partial \Psi_1}{\partial T} - \frac{\beta}{2}\frac{\partial^2 \Psi_1}{\partial \tau^2} + |\Psi_1|^2\Psi_1 = R[\Psi_0,\Psi_1]. \tag{5}$$

Here, the perturbative term R describing deviations of Eq. (5) from the integrable NLSE has a form

$$R = (-i+\zeta_0)\Psi_1 - 2|\Psi_0|^2\Psi_1 - 2\Psi_0|\Psi_1|^2 - \Psi_0^2\Psi_1^* - \Psi_0^*\Psi_1^2.$$

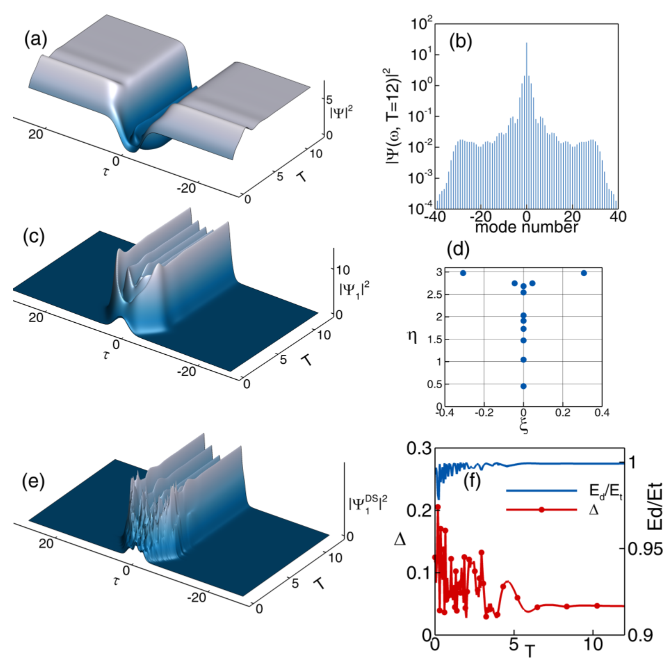

FIG. 1. Dissipative dark soliton on the stable cw background: (a) evolution with T of the intensity, $|\Psi(T,\tau)|^2$, (b) the spectral power density $|\Psi(T=12,\omega)|^2$, (c) intensity of the field without background, $|\Psi_1(T,\tau)|^2$, (d) the nonlinear discrete spectrum at $T = 12$, (e) the field reconstructed from the discrete spectrum only, $|\Psi_1^{(DS)}(T,\tau)|^2$, (f) the blue line shows the evolution with T of the fraction of energy in the discrete spectrum, $E_d(T)/E_t(T)$; the red line shows the relative integral L_2-norm of the difference between the field Ψ_1 and the field $\Psi_1^{(DS)}$ reconstructed from the nonlinear discrete spectrum. Here, $\Psi(T=0,\tau) = 2 - 1.8\exp[-(\tau/3.1)^2]$, $\beta = 1$, $\zeta_0 = 6$, $f^2 = 8.5$.

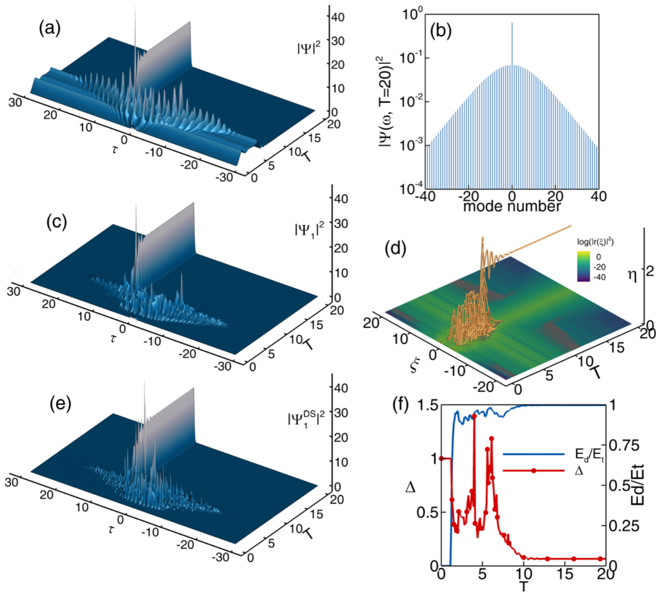

FIG. 2. Formation of the comb through the modulation instability with switched detuning: (a) full field with background, $|\Psi(T,\tau)|^2$, (b) comb spectral power density $|\Psi(T=12,\omega)|^2$, (c) $|\Psi_1(T,\tau)|^2$, (d) dynamics of the nonlinear spectrum with T shown in the complex plane $\lambda=\xi+i\eta$: the discrete spectrum (upper part) and the logarithm of $|r(\xi)|^2$ for the continuous spectrum (contour plot), (e) the field reconstructed from the discrete spectrum only, $|\Psi_1^{(DS)}(T,\tau)|^2$, (f) the blue line shows the evolution with T of $E_d(T)/E_t(T)$; the red line shows the relative integral L_2-norm of the difference between the field Ψ_1 and the field $\Psi_1^{(DS)}$ reconstructed from the nonlinear discrete spectrum. Here, $\zeta_0=2$ for $T<5$ and $\zeta_0=8.7666$ for $T\geqslant 5$. Also, $\beta=-1$, $f^2=3$, $\Psi(T=0,\tau)=1.8\exp(-2\tau^2)\cos(0.3+5\tau)$.

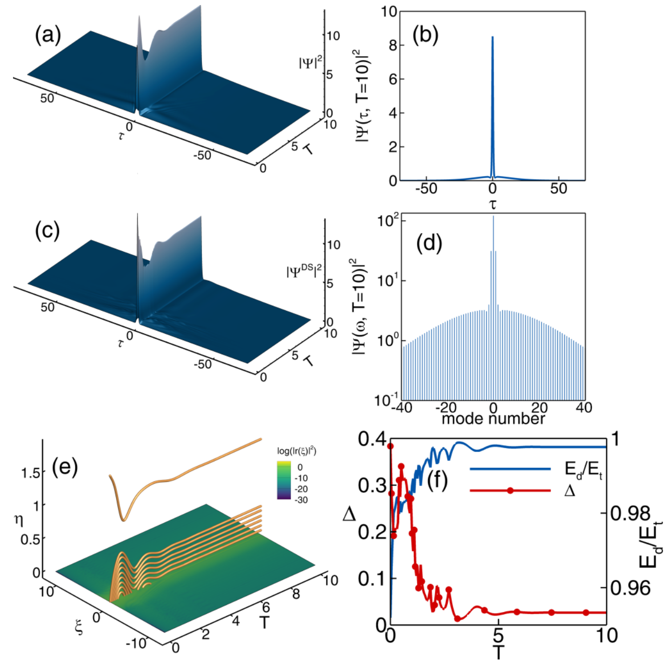

FIG. 3. Comb generation with a pulsed pumping wave [$f(\tau)=1.9\,\mathrm{sech}(\tau/20)$] generated from the Gaussian pulse $3\exp(-\tau^2/2)$: (a) dynamics of intensity, $|\Psi(T,\tau)|^2$, (b) formed comb shown at $T=10$ $|\Psi(T=10,\tau)|^2$, (c) the field $|\Psi^{(DS)}(\tau,T)|^2$ reconstructed from the discrete spectrum shown in (e), (d) the spectral power density of the comb, $|\Psi(T=12,\omega)|^2$, (e) dynamics of the nonlinear spectrum shown as the evolution with T in the complex plane $\lambda=\xi+i\eta$: the discrete spectrum (upper part) and the logarithm of $|r(\xi)|^2$ for the continuous spectrum (contour plot), (f) the blue line shows the evolution with T of $E_d(T)/E_t(T)$; the red line shows the relative integral L_2-norm of the difference between the field Ψ and $\Psi^{(DS)}$ reconstructed only from the nonlinear discrete spectrum. Here, $\zeta_0=4$, $\beta=-1$.

The proposed separation of the equations to the cw and solitonic parts only works when the background is stable. However, we will also show below how it can be used in the case of the unstable cw under the condition that the initial perturbation is localized in τ and the detuning parameter is switched from unstable to stable background regimes before the developing oscillations reach boundaries.

The Zakharov-Shabat problem (2) for the potential Ψ_1 has been solved numerically by a hybrid method that includes computing discrete eigenvalues using phase jump tracking [24] and their subsequent refinement based on the Newton method with the exponential scheme [25]. Solitons are the key element of the optical comb, providing for the phase locking of the spectral modes. Therefore, our NFT analysis here is focused on the solitons.

Figure 1 depicts the formation of a complex dissipative dark soliton in Eq. (1) with $\beta=1$ from the initial condition $\Psi(T=0,\tau)=2-1.8\exp[-(\tau/3.1)^2]$ [26] in the case of the stable background $I_0=4$. Figure 1 shows that ZSSP1 (with $\beta=-1$) can be employed in the case of normal dispersion ($\beta=1$) and that the dynamics of the field can be reconstructed with a reasonable accuracy from the discrete spectrum only. Figure 1(f) presents evolution with T of a fraction of the energy, $E_d(T)/E_t(T)$, contained in the discrete spectrum (blue line) and a relative error in terms of the L_2-norm of the reconstruction of the total field using only discrete eigenvalues (red line). It is seen that the dark soliton can be recovered with a good accuracy only from the discrete eigenvalues of the ZSSP1.

Next, we apply NFT characterization to the generation of an optical comb through the modulation instability of the unstable cw background induced by localized oscillations ($\beta=-1$). Figure 2 illustrates formation of the optical comb when $\zeta_0=2$ (unstable cw) for $T<5$ and $\zeta_0=8.7666$ (stable cw) for $T\geqslant 5$. We consider the localized oscillating perturbations at $T=0$ $\Psi(0,\tau)=1.8\exp(-2\tau^2)\cos(0.3+5\tau)$ that

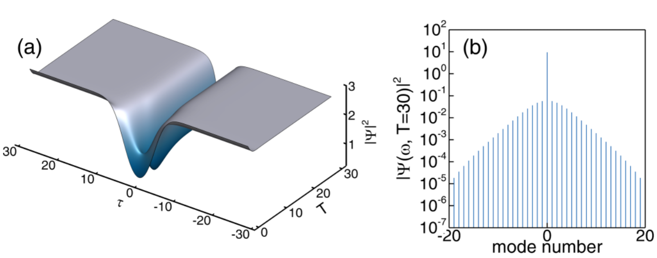

FIG. 4. Dissipative dark soliton: $\beta=1$, $\zeta_0=2.5$, $f^2=2.61$, $\Psi(T=0,\tau)=1.7-\exp[-(\tau/4.4721)^2]$. (a) $|\Psi(\tau,T)|^2$, (b) the spectral power density $|\Psi(T=30,\omega)|^2$.

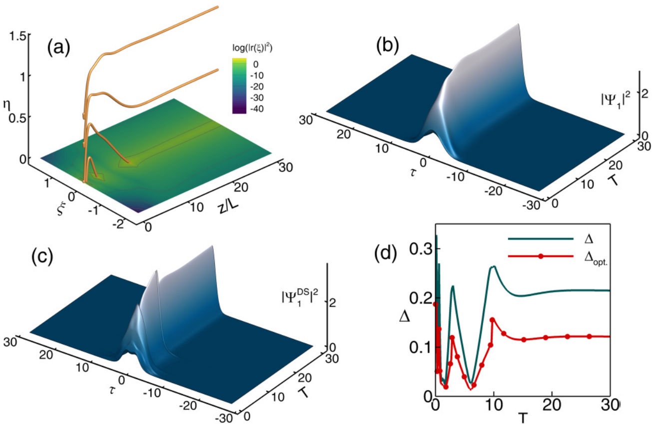

FIG. 5. Analytical approximation of dissipative dark soliton, with the same parameters as in Fig. 4. (a) Dynamics in T of the nonlinear spectrum in the complex plane $\lambda = \xi + i\eta$: the discrete spectrum (upper part) and the logarithm of $|r(\xi)|^2$ for the continuous spectrum (contour plot), (b) solution of Eq. (5) $|\Psi_1(T,\tau)|^2$, (c) the field $|\Psi_1^{(DS)}(T,\tau)|^2$ reconstructed from the discrete spectrum using the L_2-optimization procedure, (d) relative integral L_2-norm of the difference between the field Ψ_1 and the field $\Psi_1^{(DS)}$ reconstructed from the nonlinear discrete spectrum using the general procedure (purple line) and using the L_2-optimization procedure (red line).

induce instability of the background. However, before oscillations reach the boundaries in the LLE model, the detuning ζ_0 is switched to the stable cw background condition. As it is seen in Fig. 2, in the considered example, two discrete eigenvalues allow us to reconstruct the total field with relatively good accuracy.

The proposed NFT analysis is well suited to optical comb generation [27] with a pulsed pumping wave. In this case, there is no need to subtract the cw background as the boundary conditions are decaying at large $|\tau|$. Consider the pumping wave in the form of well-separated pulses of the form of $f(\tau) = 1.9\,\mathrm{sech}(\tau/20)$, similar to the example studied in [27]. Figure 3 presents NFT characterization of a comb formation from the initial Gaussian pulse, $3\exp(-\tau^2/2)$. The steady-state field [Fig. 3(b)] has well-pronounced tails, leading to a discrete spectrum with one detached eigenvalue and a set of equally spaced eigenvalues with lower imaginary parts.

Finally, considering, as an example, a single dissipative dark soliton comb (different from the one discussed in Fig. 1) studied in [26], we demonstrate that the NFT approach can provide an analytical description for such stationary coherent structures in the nonintegrable models, as shown in Fig. 4. First, the optical field in the temporal domain was restored from the two evaluated numerically discrete eigenvalues shown in Fig. 5(c) using the Darboux method. The analytical two-soliton solution of NLSE corresponding to two discrete eigenvalues has the well-known exact form [17]

$$\Psi^{(2)}(\tau) = -2\,\langle \mathbf{A}(\tau)|\,[\mathbf{I} + \mathbf{M}(\tau)^*\,\mathbf{M}(\tau)]^{-1}\,|\mathbf{B}(\tau)\rangle\,. \quad (6)$$

Here, $\mathbf{I}$ is the 2×2 identity matrix, $\mathbf{M}_{k,j}(\tau) = ir_j\frac{e^{-i(\lambda_k^*-\lambda_j)\tau}}{\lambda_k^*-\lambda_j}$, and the two-component vectors $\mathbf{A}(\tau)$ and $\mathbf{B}(\tau)$ are defined as $\langle\mathbf{A}(\tau)| = \langle r_1e^{i\lambda_1\tau}, r_2e^{i\lambda_1\tau}|$, $\langle\mathbf{B}(\tau)| = \langle e^{i\lambda_1\tau}, e^{i\lambda_1\tau}|$. For the example considered in Fig. 5, $r_1 = 2.8661 + 7.4679i$, $r_2 = 3.2519 + 2.3445i$, $\lambda_1 = 1.4085i$, and $\lambda_2 = 0.6438i$. The potential $\Psi^{(DS)}$ reconstructed from two eigenvalues provides an analytical approximation of the dissipative dark soliton given in Fig. 4(a): $\Psi(T,\tau) = \Psi_0(T,\tau) + \Psi^{(DS)}(T,\tau)$.

Though a straightforward reconstruction of the potential $\Psi_1(T,\tau)$ from the discrete spectrum of ZSSP (2) allows an approximation of the original field with good accuracy, it has disadvantages in the form of asymmetry (the original field is symmetric in τ). The reconstruction is enhanced by additional signal processing, the discussion of which is beyond the scope of this work. Here, we apply the Levenberg-Marquardt algorithm to minimize the L_2-norm of the deviation between the original and reconstructed fields. This approach makes it possible to obtain a symmetric field and to halve the L_2-error [Fig. 5(d)]. The optimal parameters read $r_1 = 2.0767 + 5.198i$, $r_2 = 1.9037 + 0.84997i$, $\lambda_1 = 1.2797i$, and $\lambda_2 = 0.47663i$ for $T = 30$. We would like to stress that the analytical formula (6) well approximates the dissipative dark soliton in the nonintegral system here, as seen in Fig. 5. Though, in this case, it is not necessary to solve the direct ZSSP, the computed discrete spectrum provides a useful initial approximation for the optimization method. We also note that the number of discrete eigenvalues in this approach can be selected from the requirements of the reconstruction accuracy.

In conclusion, we demonstrated that the NFT method based on the Zakharov-Shabat spectral problem used in the IST for NLSE with anomalous dispersion can be applied to the characterization of optical combs in systems with both anomalous and normal dispersion, and with constant or pulsed pumping wave. We have shown that the NFT technique can be used to analyze comb generation by the modulation instability of the plane wave when the detuning parameter is switched from an initially unstable background to the stable one. In the considered examples, the NFT approach allowed us to present the generated optical comb by several discrete eigenvalues. We demonstrated that NFT can provide an analytical description for some classes of dissipative dark solitons in situations when most of the energy is contained in the discrete eigenvalues. Note the interesting link to the use of a breather solution of NLSE for comb generation in Ref. [28].

This work was supported by the Russian Science Foundation (Grant No. 17-72-30006).

[1] K. Vahala, Nature (London) **424**, 839 (2003).

[2] T. J. Kippenberg, A. L. Gaeta, M. Lipson, and M. L. Gorodetsky, Science **361**, eaan8083 (2018).

[3] L. Lugiato, F. Prati, M. L. Gorodetsky, and T. J. Kippenberg, Philos. Trans. R. Soc. A **376** (2018).

[4] E. P. Grelu, *Nonlinear Optical Cavity Dynamics: From Microresonators to Fiber Lasers* (Wiley-VCH, Hoboken, NJ, 2015).

[5] T. Hansson, D. Modotto, and S. Wabnitz, Phys. Rev. A **88**, 023819 (2013).

[6] X. Xue, M. Qi, and A. M. Weiner, Nanophotonics **5**, 244 (2016).
[7] T. Hansson and S. Wabnitz, Nanophotonics **5**, 231 (2016).
[8] J. Pfeifle, V. Brasch, M. Lauermann, D. W. Yimin Yu, T. Herr, K. Hartinger, P. Schindler, J. Li, D. Hillerkuss, R. Schmogrow, C. Weimann, R. Holzwarth, W. Freude, J. Leuthold, T. J. Kippenberg, and C. Koos, Nat. Photon. **8**, 375 (2014).
[9] Óskar B. Helgason, A. Fülöp, J. Schröder, P. A. Andrekson, A. M. Weiner, and V. Torres-Company, J. Opt. Soc. Am. B **36**, 2013 (2019).
[10] S. Coen, H. G. Randle, T. Sylvestre, and M. Erkintalo, Opt. Lett. **38**, 37 (2013).
[11] I. V. Barashenkov and Y. S. Smirnov, Phys. Rev. E **54**, 5707 (1996).
[12] L. A. Lugiato and R. Lefever, Phys. Rev. Lett. **58**, 2209 (1987).
[13] K. Nozaki and N. Bekki, Physica D **21**, 381 (1986).
[14] M. Haelterman, S. Trillo, and S. Wabnitz, Opt. Lett. **17**, 745 (1992).
[15] V. F. Zakharov and A. B. Shabat, J. Expt. Theor. Phys. **34**, 62-69 (1972).
[16] M. J. Ablowitz, D. J. Kaup, A. C. Newell, and H. Segur, Stud. Appl. Math. **53**, 249 (1974).
[17] J. G. L. Lamb, *Elements of Soliton Theory* (Wiley, New York, 1980).
[18] M. J. Ablowitz and H. Segur, *Solitons and the Inverse Scattering Transform* (SIAM, Philadelphia, 1981).
[19] I. S. Chekhovskoy, O. V. Shtyrina, M. P. Fedoruk, S. B. Medvedev, and S. K. Turitsyn, Phys. Rev. Lett. **122**, 153901 (2019).
[20] P. Ryczkowski, M. Närhi, C. Billet, J.-M. Merolla, G. Genty, and J. M. Dudley, Nat. Photon. **12**, 221 (2018).
[21] S. Sugavanam, M. K. Kopae, J. Peng, J. E. Prilepsky, and S. K. Turitsyn, Nat. Commun. **10**, 5663 (2019).
[22] S. K. Turitsyn, I. S. Chekhovskoy, and M. P. Fedoruk, Opt. Lett. **45**, 3059 (2020).
[23] J. Wang, A.-G. Sheng, X. Huang, R.-Y. Li, and G.-Q. He, Chin. Phys. B **29**, 34207 (2020).
[24] I. Chekhovskoy, S. B. Medvedev, I. A. Vaseva, E. V. Sedov, and M. P. Fedoruk, Commun. Nonlinear Sci. Numer. Simul. **96**, 105718 (2021).
[25] S. Medvedev, I. Vaseva, I. Chekhovskoy, and M. Fedoruk, Opt. Express **28**, 20 (2020).
[26] C. Godey, I. V. Balakireva, A. Coillet, and Y. K. Chembo, Phys. Rev. A **89**, 063814 (2014).
[27] M. Malinowski, A. Rao, P. Delfyett, and S. Fathpour, APL Photon. **2**, 066101 (2017).
[28] B. Frisquet, A. Chabchoub, J. Fatome, C. Finot, B. Kibler, and G. Millot, Phys. Rev. A **89**, 023821 (2014).